3-Dimensional Blood Cooling Model inside a Carotid Bifurcation

Ryan Sikorski*[1], Thomas Merrill[1]
[1]Department of Mechanical Engineering – Rowan University
*Corresponding author: sikors95@students.rowan.edu

Stroke is caused by an interruption of brain blood supply and is one of the leading causes of death and disability. A mild reduction of 2-5°C in tissue temperature through hypothermia has shown reduced tissue infarct size, increased tissue recovery, and positive neurological effects. This paper seeks to predict the outlet blood temperature in the common carotid bifurcation branches. In our model a catheter injects cooled blood into the carotid artery bifurcation with a constant artery wall temperature. Final model simulations show outlet temperatures of the carotid bifurcation branches with varying artery inlet flow rates. Simulating the effect of cooling in the common carotid bifurcation allows future work in predicting brain tissue hypothermia potential and more advanced brain tissue thermal simulations.

Keywords: Bioengineering, Fluid Mechanics, Heat Transfer, Hypothermia, Blood Cooling.

1. Introduction and Background

Stroke is caused by an interruption of brain blood supply and is one of the leading causes of death and disability in the world [1]. The ability to rapidly induce localized mild hypothermia has proven benefits in reduction of tissue death from an ischemic stroke, which account for 87% of all strokes [2]. A mild reduction of 2-5°C in tissue temperature has shown reduced tissue infarct size, increased tissue recovery, and positive neurological effects [3,4]. This paper seeks to predict the outlet temperatures in the bifurcation branches of the common carotid artery. Simulating the effect of cooling in the common carotid bifurcation through Computational Fluid Dynamics (CFD) software allows future work in predicting deep brain tissue hypothermia penetration.

Therapeutic hypothermia (TH) is a new treatment that reduces a patient's temperature to induce mild to moderate levels of hypothermia (2-5°C reduction in tissue temperature) throughout the entire body or at specific organs. The objective of TH is a reduction or elimination of reperfusion injury associated with re-establishing blood flow to an ischemic organ. Therapeutic hypothermia has already proven benefits in the applications of cardiac arrest in numerous research journals and clinical studies [5,6]. Current treatments such as cooling caps, blankets, and ice bathes lack the ability to deliver rapid localized cooling to organs.

Current mechanical thrombectomy devices such as the Concentric Merci Retriever [7] remove a neurovasculature blockage but do not couple with hypothermia solutions. A unique blood cooling system may be coupled with similar devices into a single tissue salvage solution. This combination has delivered rapid brain tissue cooling - up to 8°C in under 5 minutes during canine testing [8].

2. Governing Equations and Models

2.1 Validation of COMSOL Software:

Modeling practices and software were validated through comparison with analytical solutions. Fluid flow was validated by measuring pressure drop and mass balance using the *Steady State Laminar Flow* module. The inlet tube velocity was calculated by setting a constant flow rate with a fixed cross-sectional area using Q=VA, where Q is volumetric flow rate, A the area, and V is the inlet velocity

Reynolds number was calculated from Eq. (1) where ρ, V, D, and μ are fluid density, inlet velocity, tube diameter, and dynamic viscosity. Flows with a Reynolds number less than 2300 are considered fully laminar [9].

$$Re_D = \frac{\rho V D}{\mu} \quad (1)$$

Pressure drop across the tube was calculated using the Poiseuille equation Eq. (2), where μ, L, Q, and r are the dynamic viscosity, tube length, volumetric flow rate, and radius.

$$\Delta P = \frac{8\mu L Q}{\pi r^4} \quad (2)$$

The model used material properties of water at 37°C, a length of 0.106 m, diameter of 6.5E-3m, inlet velocity of 0.22 m/s, with a no slip condition along the walls, and zero pressure at

the outlet. A *physics generated* mesh was applied, consisting of 542,000 elements. COMSOL predicted the pressure drop with an error of 0.20% from the analytical calculation. A mass balance was performed on the inlet and outlet with an error of 0.001%.

The same geometry, materials, meshing, and flow boundary conditions were applied to a heat transfer model using the *Non-Isothermal Flow* module. A consistent surface temperature was prescribed at the walls, and a zero temperature gradient at the outlet. Temperature change along an axis of a tube with developing laminar flow and constant surface temperature were predicted by Eq. (3). Where T_s is the surface temperature, $T_{m,o}$ is the mean outlet temperature, $T_{m,i}$ is the mean inlet temperature, P is the tube perimeter, $\dot{m}$ is the mass flow rate, C_p is specific heat capacity, and $\bar{h}$ is the average heat transfer coefficient along the tube.

$$\frac{T_S - T_{m,o}}{T_s - T_{m,i}} = exp\left(-\frac{Px}{\dot{m}C_p}\bar{h}\right) \quad (3)$$

Eq. (4) defines the Prandlt number which was solved into Eq. (5) that defines the average heat transfer coefficient in this case.

$$Pr = \frac{C_p\mu}{k} \quad (4)$$

$$\overline{Nu_D} \equiv \frac{\bar{h}D}{k} = 1.86\left(\frac{Re_D Pr}{L/D}\right)^{1/3}\left(\frac{\mu}{\mu_s}\right)^{0.14} \quad (5)$$

The mean outlet temperature in COMSOL was simulated with an error of 0.09% from the analytical calculation, the mass balance and pressure drop error remained consistent with the isothermal case.

2.2 Bifurcation Model:

To validate bifurcation models a 3D *symmetric* 45° angle bifurcation was simulated to estimate the flow, pressure, temperature, and geometry characteristics of the final model. Figure 1 shows a symmetric arterial bifurcation with the initial branch designated as P0, and each branch of the bifurcation as P1 and P2.

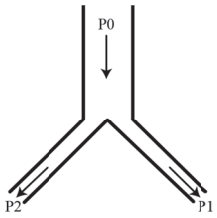

Figure 1: A symmetric bifurcation diagram, showing parent and two branches.

Flow in a symmetric bifurcation follows the principles of the Poiseuille equation presented in Eq. (2). The pressure drop was first calculated in P0 branch, then in each respective bifurcated branch P1 and P2. The flow rate from P1 and P2 was estimated to each be ½ the flow rate of P0. The total pressure drop across a bifurcation branch is then determined by the sum of P0 and P1 or P2. This is an idealized simplistic case that relies on the assumption of steady laminar flow, in a rigid tube. Inlet boundary conditions of pressure, velocity, and mass flow rate were simulated in a laminar flow CFD simulation with a mean difference of 0.77% from analytically calculated values.

An *asymmetric* bifurcated steady state flow in rigid tubes can be defined by the introduction of a bifurcation index in Eq. (6), relating the radii of each bifurcation branch.

$$\alpha = \frac{a_2}{a_1} \quad (6)$$

The flow rate in asymmetric branches can be determined by simultaneous solving of Eq. (7) and Eq. (8) by inserting the previously solved bifurcation index.

$$\frac{a_0}{a_x} = (1 + \alpha^\gamma)^{\frac{1}{\gamma}} \quad (7)$$

$$q_x \approx a_x^\gamma \quad (8)$$

2.3 Temperature predication with catheter:

A catheter injects fluid along the centerline axis of a three dimensional tube with assumed constant surface temperature. The catheter has an insert length 1/14th of the total tube length. The flow, geometry, material, and heat transfer boundary conditions are the same as the models presented in section 2.1. Additionally, a no slip is applied to the catheter walls, with a constant inlet temperature. A total number of 638,000 mesh elements were used.

The combined volumetric flow rate of the catheter and artery determine a mean fully developed velocity, Reynolds number, and Prandlt number. Using these values produces the mean outlet temperature. The mean difference between the models and analytical: outlet temperature 0.15%, pressure drop 1.65%, and outlet flow rate 3.0%.

3. Methods and use of COMSOL for Final Model

3.1 Geometry:

The final model was constructed 3-Dimensionally in SolidWorks and imported into COMSOL using LiveLink capabilities. Initial geometric values were informed by the work of Perktold [11], and adjusted based on the mean values from studies of healthy adults to account for variations [12,13]. The model is constructed with dimensions as shown in Table 1 corresponding to locations in Figure 2. The length of CCA was made sufficiently long to allow for full mixing of the fluid. The model is an idealized mock artery that does not account for curvature of the artery branches, torosity, and surrounding tissue.

The 6F (2.0E-3 m) catheter was modeled as an extruded cut with an inner diameter of 1.8E-3 m and a length 1/14th that of the CCA. This allowed flow modeling analytically to be modeled as flow through a tube not an annulus, it is assumed that the catheter enters the body prior to the geometry, and only the tip of the catheter is modeled. The wall thickness of the catheter was negated.

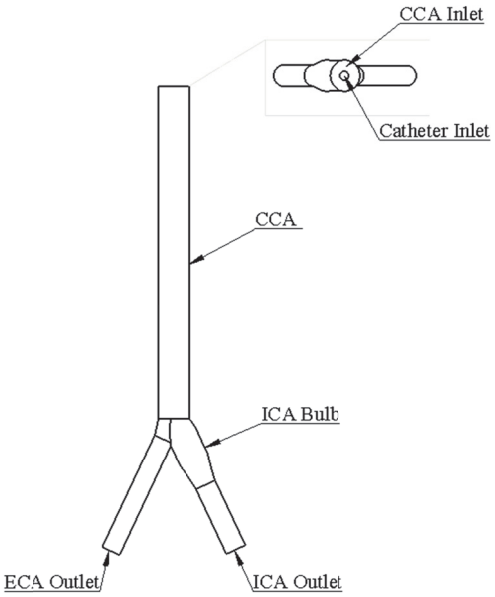

Figure 2: Final model in a top down line drawing view, with side view of catheter insertion.

Table 1: Geometry values for final 3D model.

Geometry	*Value(mm)*
CCA Length	70.0
CCA Diameter	6.5
Catheter Length	5.0
Catheter Diameter	1.8
ICA Length	30.0
ICA Diameter	4.4
ICA Bulb Max Diameter	6.5
ECA Length	30.0
ECA Diameter	4.0
ICA/ECA Angle to CCA Centerline	25°

3.2 Fluid Properties:

The properties were based on the fluid and thermal properties of blood, shown in Table 1. Blood may behave as a Non-Newtonian fluid, however the fluid was assumed to act Newtonian based on the arterial sizes being much larger than that of a typical red blood cell (7μm), and above the threshold of 1mm [14].

Table 2: Fluid and thermal properties of blood.

Property	*Value*	*Source*
Density	1060[kg/m^3]	[9]
Dynamic Viscosity	0.0035[Pa*s]	[15]
Thermal Conductivity	0.492[W/(m*K)]	[16]
Specific Heat	3600[J/(kg*K)]	[16]

3.3 Boundary Conditions and Solver:

Boundary conditions for flow and heat transfer were prescribed to the model as show in Table 2. A default GMRES iteration based solver was used for all modeling. The *Non-Isothermal Flow* module was used in version 4.2 of COMSOL.

Table 3: Flow and heat transfer boundary conditions.

Boundary	*Condition*	*Value*
Artery Inlet	Mass Flow Rate	4.5 ml/s – 8.5 ml/s
Catheter Inlet	Mass Flow Rate	2.65E-3 [kg/s]
ICA Outlet	Pressure No Viscous	0 [Pa]
ECA Outlet	Pressure No Viscous	0 [Pa]
Remaining Boundaries	No Slip	-
Artery Inlet Temperature	Temperature	310 [K]
Catheter Inlet/Wall Temperature	Temperature	301 [K]
Wall Temperature	Temperature	310 [K]
ICA & ECA Outflow	Normal Temperature Gradient = 0	-

The artery inlet varied by setting the input to a parameter and performing a parametric sweep. The inlet boundary conditions of the artery are assumed to be steady state using a mean flow rate. This assumption is physiologically false as the human heart produces a waveform resulting in pulsatile flow in the arterial network. However, since the objective was to determine the effects of cooling averaged over a long period of time, the steady flow assumption may prove to be valid. Artery inlet temperature is based on average core temperature of the human body prior to hypothermia treatment.

Catheter inlet and temperature was determined through previous work [8]. The exterior walls of the catheter were set to a no slip condition. Outlets of the ICA and ECA were set to a zero pressure no viscous forces condition, with a zero temperature gradient at outlet.

3.4 Meshing and Mesh Convergence:

A mesh convergence study was completed using pressure drop and mean outlet temperature of the ICA branch as convergence criteria; pressure drop is shown in Figure 3. The final model has 757,000 tetrahedral elements, 102,000 prism elements, and 860,000 total elements. The mesh was generated use the '*Physics Based Mesh – Fine*r' setting within COMSOL.

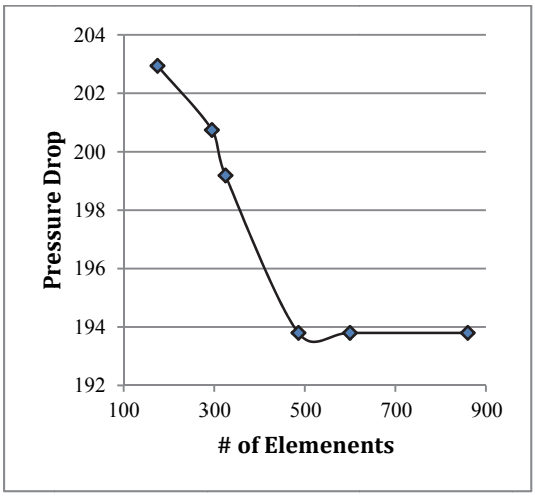

Figure 3: Final model mesh convergence study based on pressure drop.

4. Results

A mean blood flow rate of 7.5E-6 m^3/s was determined by existing literature on healthy adults[13]. This blood flow rate was run for models presented in sections 4.1 and 4.2..

4.1 Velocity and Pressure Distribution:

Figure 4 shows the velocity distribution in the bifurcation. A pressure maxima occurs between the ICA and ECA branches, this corresponds with other literature [15].

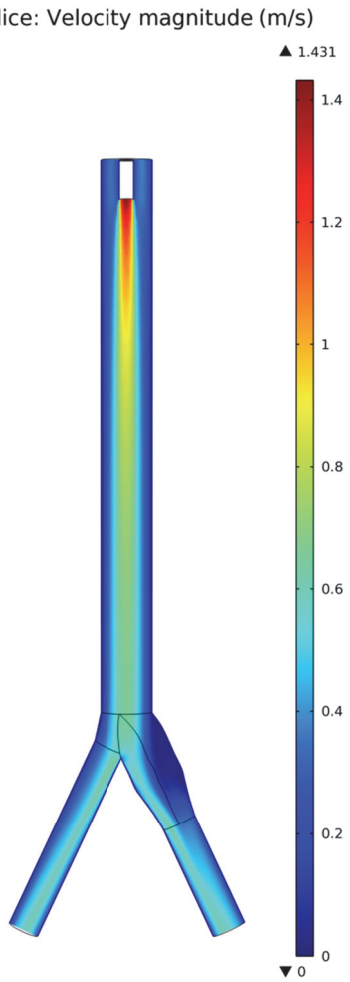

Figure 4: Velocity distribution along the centerline plane axis, as presented in a top down view.

4.2 Temperature Distribution:

Figure 5 shows the temperature distribution along the centerline axis. A higher mean velocity along the inner walls of the ICA and ECA branch, Figure 4 causes an increase in heat transfer coefficient (h). The constant wall temperature implies an infinite thermal capacitance for the surrounding tissue.

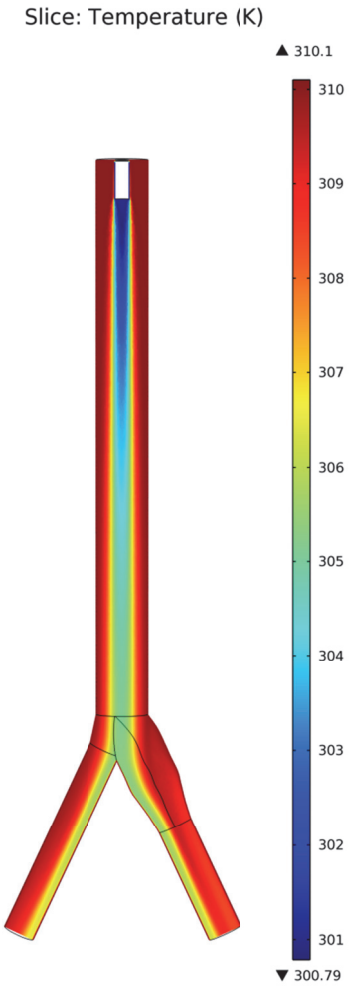

Figure 5: Temperature distribution along the centerline plane axis, as presented in a top down view.

4.3 Artery Inlet Parametric Study:

The final model was also run using a parametric study by varying artery inlet blood flow rates. The flows ranged in value from 4.5 ml/s to 8.5 ml/s.

Figure 6 shows the temperature distribution at the point in the CCA directly prior to the bifurcation. Figures 7 and 8 show the outlet temperature distribution of the ICA and ECA at flow rates of 4.5 ml/s and 8.5 ml/s. Figure 9 shows the temperature distribution for blood flow rates in the ICA and ECA varied parametrically from 4.5 ml/s to 8.5 ml/s

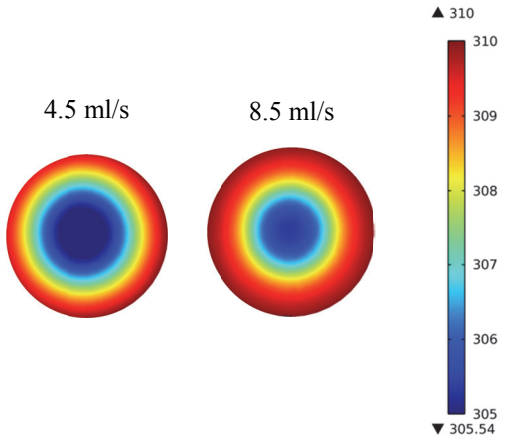

Figure 6: Temperature distribution of CCA directly prior to bifurcation with two flow rates.

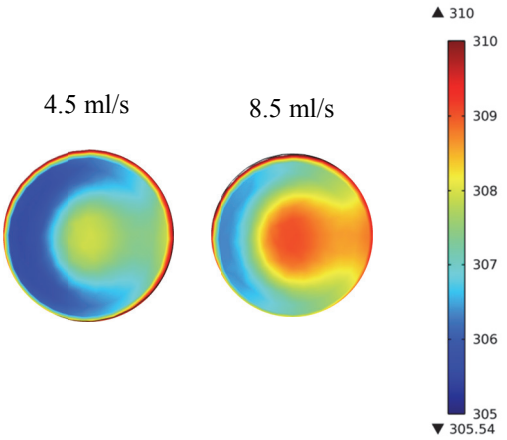

Figure 7: Temperature distribution of ICA outlet with two flow rates.

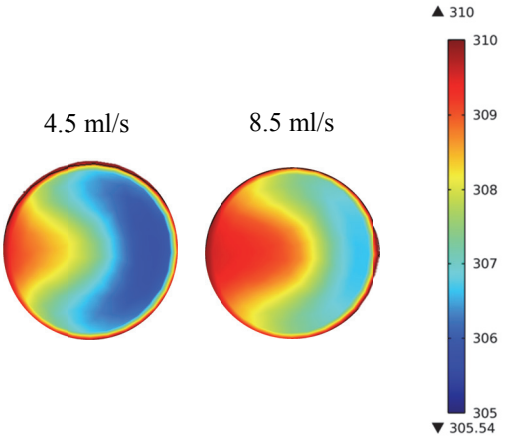

Figure 8: Temperature distribution of ECA outlet with two flow rates.

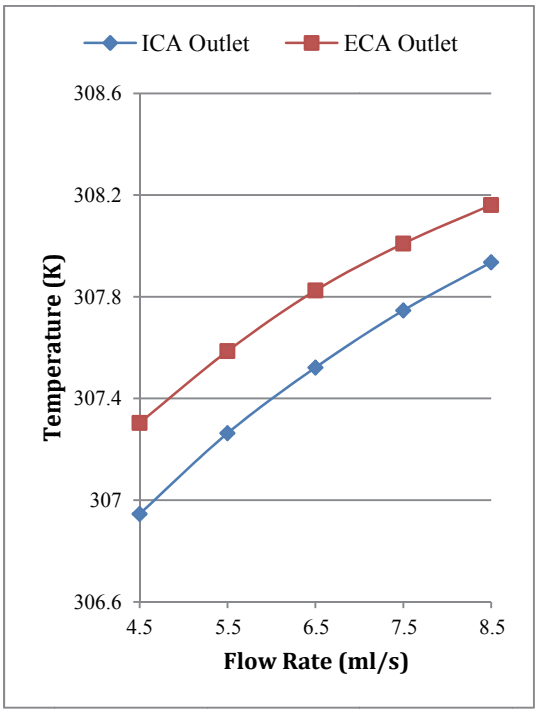

Figure 9: Temperature distribution of ECA and ICA outlet with two blood flow rates.

5. Discussion and Future Work

The correlation between artery flow rate and temperature at the ICA and ECA outlets shows a decrease in cooling as artery flow rate rises. We successfully predict the outlet temperatures in the carotid bifurcation based on an assumed constant artery wall temperature. The modeling and data gathered here will be used to inform more detailed models of the carotid bifurcation, and the cerebral arterial network. Ultimately we seek to determine the ability for cooled blood to remove thermal energy from surrounding brain tissue.

Future work on the this model will include understanding the effect of pulsatile vs. steady state flow conditions, heat transfer through conduction to surrounding tissue, and a detailed anatomical model provided through scanned imaging techniques.

References:

[1] World Health Orgnazation, 2011, "The top 10 causes of death," [1] "The top 10 causes of death." [Online]. Available: http://www.who.int/mediacentre/factsheets/fs310/en/index.html. [Accessed: 28-Feb-2012].

[2] Lloyd-Jones D., Adams R., Carnethon M., De Simone G., Ferguson T. B., Flegal K., Ford E., Furie K., Go A., Greenlund K., Haase N., Hailpern S., Ho M., Howard V., Kissela B., Kittner S., Lackland D., Lisabeth L., Marelli A., McDermott M., Meigs J., Mozaffarian D., Nichol G., O'Donnell C., Roger V., Rosamond W., Sacco R., Sorlie P., Stafford R., Steinberger J., Thom T., Wasserthiel-Smoller S., Wong N., Wylie-Rosett J., and Hong Y., 2009, "Heart disease and stroke statistics--2009 update: a report from the American Heart Association Statistics Committee and Stroke Statistics Subcommittee.," Circulation, **119**(3), pp. 480–6.

[3] Holzer M., Bernard S. a., Hachimi-Idrissi S., Roine R. O., Sterz F., and Millner M., 2005, "Hypothermia for neuroprotection after cardiac arrest: Systematic review and individual patient data meta-analysis," Critical Care Medicine, **33**(2), pp. 414–418.

[4] van der Worp H. B., Sena E. S., Donnan G. a, Howells D. W., and Macleod M. R., 2007, "Hypothermia in animal models of acute ischaemic stroke: a systematic review and meta-analysis.," Brain : a journal of neurology, **130**(Pt 12), pp. 63–74.

[5] Bernard S. A., Gray T. W., Buist M. D., Jones M., Silvvester W., Gutteride G., and Smith K., 2002, "Treatment of comatose survivors of outof-hospital cardiac arrest with induced hypothermia," New England Journal of Medicine, (346), pp. 557–563.

[6] Holzer M., Cerchiara E., Martens P., and et al., 2002, "The Hypothermia After Cardiac Arrest Study Group. Mild Therapeutic Hypothermia to Improve the Neurologic Outcome After Cardiac Arrest," New England Journal of Medicine, **346**, pp. 549–556.

[7] Smith W. S., Sung G., Saver J., Budzik R., Duckwiler G., Liebeskind D. S., Lutsep H. L., Rymer M. M., Higashida R. T., Starkman S., Gobin Y. P., Frei D., Grobelny T., Hellinger F., Huddle D., Kidwell C., Koroshetz W., Marks M., Nesbit G., and Silverman I. E., 2008, "Mechanical thrombectomy for acute ischemic stroke: final results of the Multi MERCI trial.," Stroke; a journal of cerebral circulation, **39**(4), pp. 1205–12.

[8] Merrill T., Merrill D. R., and Akers J., 2012, "Localized Brain Tissue cooling For Use During Intracranial Thrombectomy." SBC2012-80833, American Society of Mechanical Engineering (ASME) 2012 Summer Biomedical Engineering Conference, Fajardo, Puerto Rico, June 20-23, 2012.

[9] Okiishi T., Munson B., and Young D., 1998, Fundamentals of Fluid Mechanics, John Wiley & Sons, Inc., New York, NY.

[10] Zamir M., 2005, The Physics of Coronary Blood Flow, Springer, New York, NY.

[11] Perktold K., and Rappitsch G., 1995, "Computer simulation of local blood flow and vessel mechanics in a compliant carotid artery bifurcation model.," Journal of biomechanics, (7), pp. 845–56.

[12] Krejza J., Arkuszewski M., Kasner S. E., Weigele J., Ustymowicz A., Hurst R. W., Cucchiara B. L., and Messe S. R., 2006, "Carotid artery diameter in men and women and the relation to body and neck size.," Stroke; a journal of cerebral circulation, **37**(4), pp. 1103–5.

[13] Markl M., Wegent F., Zech T., Bauer S., Strecker C., Schumacher M., Weiller C., Hennig J., and Harloff A., 2010, "In vivo wall shear stress distribution in the carotid artery: effect of bifurcation geometry, internal carotid artery stenosis, and recanalization therapy.," Circulation. Cardiovascular imaging, **3**(6), pp. 647–55.

[14] Waite L., and Fine J., 2007, Applied Biofluid Mechanics, McGraw-Hill, New York, NY.

[15] Perktold K., Resch M., and Florian H., 1991, "Pulsatile Non-Newtonian Flow Characteristics in a 3-Dimensional Human Carotid Bifurcation," Journal of Biomechanical Engineering, (113), pp. 467–475.

[16] Diller K. R., Valvano J. W., and Pearce J. A., 1999, Handbook of Thermal Engineering.